Distillation column unit operation design

Lazenby, MM

CPJ 421

2020-10-09

Distillation column unit operation design

Matthew Lazenby
16040954

Department of Chemical Engineering
University of Pretoria
South Africa

CPJ 421

2020-10-09

Distillation column unit operation design

Executive Summary

The production of ETBE is required via the reaction of isobutene with bioethanol. The isobutene is sourced from a LPG source that derives from a fluid catalytic cracker (FCC) cut (McKinsey, 2020). The FCC cut is to be purified to separate the undesired C_3 hydrocarbons (propane and propylene) from the mixture. Table 1 specifies the feed flow rate and composition to the distillation column. The separation occurs at a high pressure of 1500 kPa and a moderate temperature of 62 °C (De Sousa Melim *et al*, 2020). The separation is a multi-component distillation with propane as the light key and isobutane as the heacy key. The multi-component feed mixture is a two-phase mixture that behaves as a non-ideal mixture, modelled using the Peng-Robinson thermodynamic model (Nasri & Housam, 2009).

The column overall efficiency was calculated to be ≈ 80 %. The column was optimised using the sensitivity analysis tool provided by DWSIM. The sensitivity analysis tool was used to optimise the reflux ratio and number of stages for the column design, followed by optimisation of the feed stage using a rigorous distillation column. This optimisation was based off of preliminary design parameters provided by results of shortcut method implementation. Table 2 provides a summary of parameters for the optimised column incorporating the overall efficiency of the column.

The column mechanical design was done based on sizing and hydraulic relations and algorithms provided in Wankat (2017) and Sinnott & Towler (2019). The material of construction is discussed in the design that follows. Table 3 details the column dimensions, plate hydraulics and plate dimensions for the column design with a selection of sieve trays as the chosen plate type. The plate hydraulics and column internal and external dimensions considers the design for entrainment, flooding, plate pressure drop and weeping. The mechanical design is aided by Figure 1. Figure 1 shows a detailed diagram of the designed distillation column that successfully separates the C_3 hydrocarbons from the C_4 hydrocarbons without compromise on the desired reactant flow rate ($F_{\text{isobutene}} = 29\,425\,\text{kmol}\,\text{hr}^{-1}$ (De Sousa Melim *et al*, 2020) – shown in Table 2). The heat exchangers required as the condenser and reboiler was designed and detailed in the report. Selection of a single shell pass and 4 tube passes, shell and tube heat exchanger was made for the condenser while the reboiler was designed to be a thermosyphon reboiler.

Table 1: Distillation column feed flow specification

Component	Mass flow ($\mathrm{kg\,hr^{-1}}$)	z
Propylene	12 015	0.1
Propane	60 071	0.47
Isobutane	1 260	0.01
Isobutene	25 878	0.16
1-butene	23 857	0.15
n-butane	5 651	0.03
Trans-2-butene	12 142	0.07
Cis-2-butene	3 302	0.02
Overall Feed	144 175	1

Table 2: Optimised, efficiency adjusted column design parameters

Property	value
N_{stages}	23
Feed stage	12
Distillate flow rate	$1666\,\mathrm{kmol\,hr^{-1}}$
Bottoms flow rate	$1262\,\mathrm{kmol\,hr^{-1}}$
$\mathrm{L}_{\mathrm{Distillate}}$	$2166\,\mathrm{kmol\,hr^{-1}}$
$\mathrm{V}_{\mathrm{Distillate}}$	$3832\,\mathrm{kmol\,hr^{-1}}$
$\mathrm{L}_{\mathrm{Bottoms}}$	$4171\,\mathrm{kmol\,hr^{-1}}$
$\mathrm{V}_{\mathrm{Bottoms}}$	$2909\,\mathrm{kmol\,hr^{-1}}$
Reflux ratio	1.3
Boil-up ratio	2.3
Isobutene flow rate (bottoms)	$24\,917\,\mathrm{kg\,hr^{-1}}$
Condenser duty	14 231 kW
Reboiler duty	−11 098 kW

Table 3: Plate hydraulics and column dimensions

Property	unit	value
Column height (H_{column})	m	35
Column diameter (D_c)	m	3.6
Column area (A_c)	m^2	10
Downcomer area (A_d)	m^2	1.2
Net area (A_n)	m^2	8.8
Active area (A_a)	m^2	7.6
Hole area (A_h)	m^2	0.38
Weir length (L_w)	m	2.8
Weir height	mm	40
Hole diameter (d_h)	mm	3
Plate thickness	mm	3
$\check{u}_h$	$m\,s^{-1}$	4.9
h_d	mm	103
h_r	mm	25.6
$h_{ow_{max}}$	mm	98.4
h_t	mm	266.6
ΔP_{plate}	kPa	1.3
h_{ap}	mm	30
A_{ap}	m^2	0.084
h_{dc}	mm	416
h_b	mm	821
t_r	s	7.4
u_v	$m\,s^{-1}$	0.21
Percent flooding	%	72.5
Liquid-vapour factor (F_{LV})		0.34
ψ		0.004

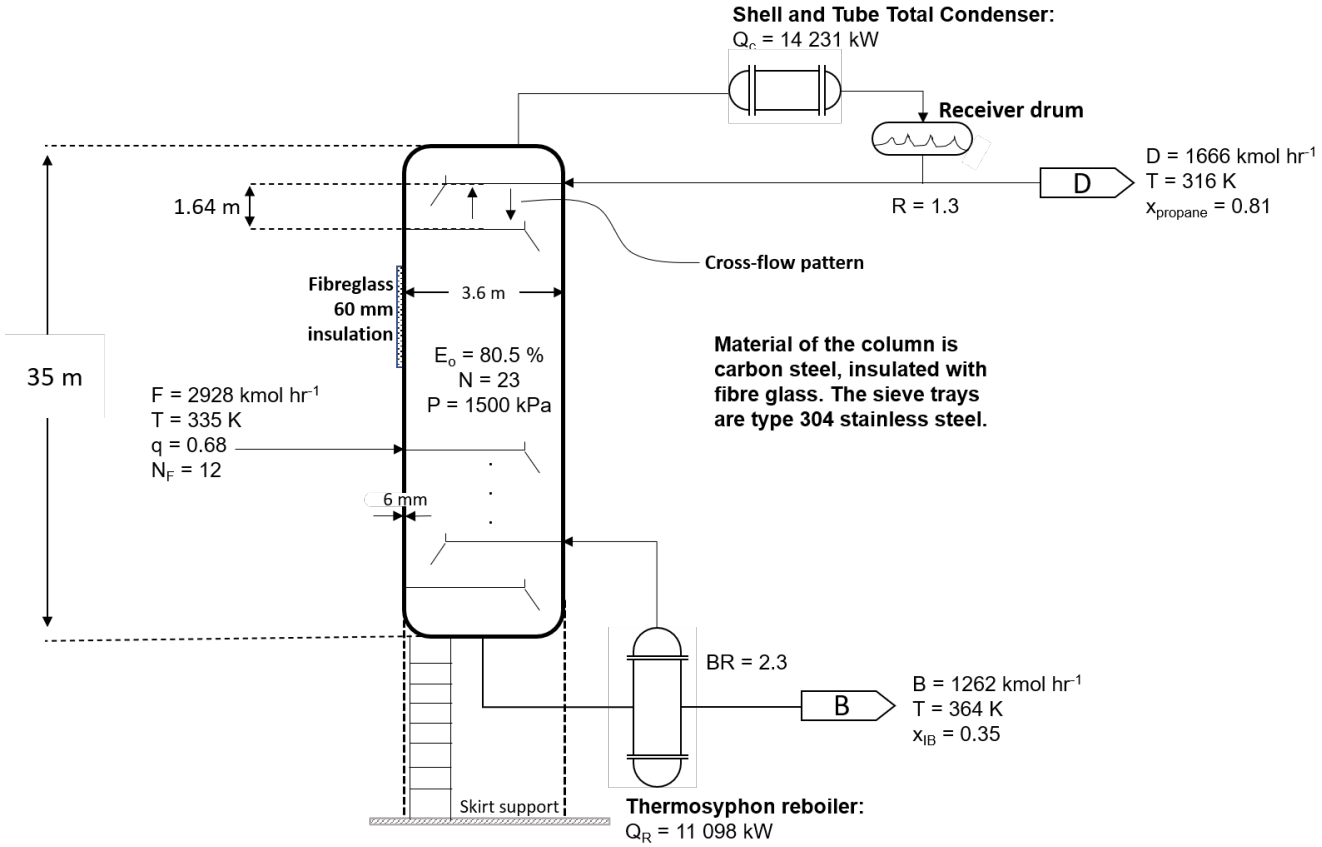

Figure 1: Plated distillation column design and dimension

Contents

Executive Summary **i**

1 Introduction **1**

2 Assumptions and physical data **1**

2.1 Assumptions 1

2.2 Physical data 2

3 Design optimisation **5**

4 Column design and calculations **11**

4.1 Efficiency 11

4.2 Column considerations and constraints 12

4.3 Column dimensions 13

4.4 Insulation 18

5 Heat exchangers **18**

5.1 Condenser 18

5.2 Reboiler 21

6 Design Detail **22**

7 References **24**

1 Introduction

A plated, simple distillation column was deigned for the separation of a C_3 and C_4 mixture. The separation involves multi-component distillation, where the desired separation is to completely separate the C_3's (propane and propylene) from the mixture. Isobutene is the desired product. Therefore, concentrating this compound in the bottoms was a important design consideration. De Sousa Melim *et al* (2020) designed for a isobutene flow rate of $24\,925\,\mathrm{kg\,hr^{-1}}$. The isobutene is fed to a reactor as valuable reactant at the specified mass flow rate for production of ETBE at around 30 tons per hour. Table 4 details the column feed specifications. The column was designed to operate at a temperature of 335 K (62 °C) and a pressure of 1500 kPa. The design aimed at minimising the capital cost while ensuring the column had no mechanical violations.

Table 4: Distillation column feed specification

Component	Mass flow ($\mathrm{kg\,hr^{-1}}$)	z
Propylene	12 015	0.1
Propane	60 071	0.47
Isobutane	1 260	0.01
Isobutene	25 878	0.16
1-butene	23 857	0.15
n-butane	5 651	0.03
Trans-2-butene	12 142	0.07
Cis-2-butene	3 302	0.02
Overall Feed	144 175	1

2 Assumptions and physical data

2.1 Assumptions

When designing a distillation column, there are a number of assumptions that need to be made to simplify the design procedure. The assumptions made for the design, to separate C_3's from C_4's, are listed below. Beginning with the most important assumption (CMO):

- For every mole of liquid that is vapourised, one mole of vapour is condensed (Constant Molar Overflow). This assumption leads to further detailed assumptions

(Wankat, 2017):

- The column is adiabatic. Therefore, heat exchange occurs only in the condenser and reboiler
- The specific heat changes are small compared to the latent heat changes
- On a per mole basis, the latent heat of vaporisation (λ) is constant
- Saturated vapour and liquid lines are parallel on the, molar unit, enthalpy composition diagram (H-xy)

- The column operates at steady-state conditions which are considered optimal
- Liquid physical properties such as density and viscosity are considered constant. Additionally, column pressure is assumed constant at 1500 kPa
- Relative volatility is considered constant for a mixture
- There exists a vapour-liquid equilibrium between vapours and liquids both entering and exiting the column.
- For a hydrocarbon mixture it is assumed that the Peng-Robinson thermodynamic model holds true (Nasri & Housam, 2009)

2.2 Physical data

The FCC raw cut that is assumed as the source of isobutene for the ETBE production, is a mixture of C_3's and C_4's. This mixture is a non-ideal mixture and therefore, a thermodynamic model is used to model the behaviour of the mixture. The thermodynamic model chosen is the Peng-Robinson model (Nasri & Housam, 2009). The separation involves multi-component distillation, a design decision had to be made as how best to separate the C_3's from the C_4's. To make this crucial design decision, the relative volatility's of the components were calculated using Equation 1 (Wankat, 2017).

$$\alpha_{AB} = \frac{\frac{y_A}{x_A}}{\frac{y_B}{x_B}} \tag{1}$$

The feed composition is given in the DWSIM simulation. Therefore, Table 5 lists the component relative volatility for the feed mixture in order of decreasing volatility. The separation of the hydrocarbons occurs between propane and isobutane. Propane, therefore, is recognised as the Light Key (LK) and isobutane as the Heavy Key (HK). Table 5

shows that:

$$\alpha_{\frac{LK}{HK}} = 2.4$$

Important to note from Table 5 is that the ease of separation between C_3's is rather difficult and this separation difficulty is further enhanced when evaluating the ease of separation for the C_4's.

Table 5: The relative volatility of the components in the feed mixture, listed in order of decreasing volatility

Component	y	x	α
Propylene	0.14	0.08	
			1.2
Propane	0.6	0.41	
			2.4
Isobutane	0.01	0.01	
			1.1
Isobutene	0.1	0.18	
			1
1-butene	0.09	0.17	
			1.2
n-butane	0.02	0.04	
			1
Trans-2-butene	0.04	0.09	
			1.1
Cis-2-butene	0.01	0.02	

The LK and HK can be considered as a binary mixture and therefore, Figure 2 is the VLE data plotted for the separation on a T-xy diagram. This diagram further supports that propane is the light key and isobutane is the heavy key. Figure 2 shows that the separation is a simple distillation and no azeotrope occurs in the distillation.

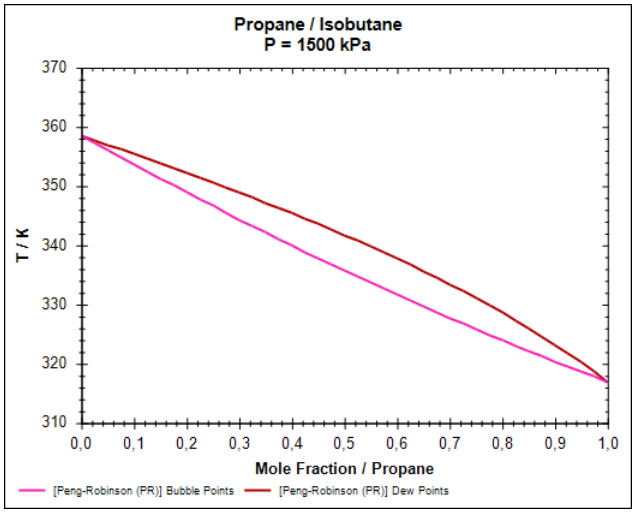

Figure 2: Temperature composition diagram for the LK and HK distillation

Further physical data as listed in Table 6 is obtained through DWSIM. The boiling point of the mixture is obtained by cloning the feed and changing the temperature of the feed until the vapour phase mole fraction just becomes zero (Figure 2). The quality of the feed is available from DWSIM (not directly). The quality is defined as: $q = (1 - \text{Vapour mole fraction})$. DWSIM provides a vapour mole fraction of 0.32 for the feed. Therefore, the quality of the feed is calculated and tabulated below. The quality proves that the feed is a two-phase mixture (vapour & liquid).

Table 6: Physical data

Property	unit	value
$\mathrm{Cp}_{feed_{mixture}}$	$\mathrm{kJ\,kg^{-1}\,K^{-1}}$	2.94
T_{feed}	K	335
$\mathrm{T}_{feed_{BP}}$	K	333.3
q_{feed}		0.68
$\mu_{feed_{mixture}}$	Pa s	5.5×10^{-5}
$\rho_{vapour_{bottom}}$	$\mathrm{kg\,m^{-3}}$	27.76
$\rho_{liquid_{bottom}}$	$\mathrm{kg\,m^{-3}}$	488
$\rho_{vapour_{dist}}$	$\mathrm{kg\,m^{-3}}$	25.12
$\rho_{liquid_{dist}}$	$\mathrm{kg\,m^{-3}}$	466
σ_{bottom}	$\mathrm{N\,m^{-1}}$	0.005
σ_{dist}	$\mathrm{N\,m^{-1}}$	0.005
$\rho_{mixture}$	$\mathrm{kg\,m^{-3}}$	74.9

3 Design optimisation

The column optimisation was achieved using the sensitivity analysis tool provided by DWSIM. However, before the optimisation and use of the sensitivity analysis initial estimates need to be calculated for the column design. These estimates are: minimum number of stages, minimum reflux ratio and feed location. There are various shortcut methods that are used to determine the initial estimates mentioned above. The most common shortcut method used in multi-component distillation is the Fenske-Underwood-Gilliland (FUG) method. Additionally, DWSIM allows for a shortcut column to be design based of the desired separation and flow rates. However, these initial estimates are to be taken with a "pinch of salt" as their results are indeed only estimates. The reason for variation in the estimates is because of the many simplifying assumptions that are made when developing the shortcut method models (Ramapriya *et al*, 2018). The multi-component distillation has an increased degrees of freedom compared to binary distillation. For a 8 component mixture, the degrees of freedom is 14 degrees of freedom. This implies that the distillate nor bottoms composition can be completely specified due to the additional degrees of freedom. This adds calculation complexities and thus affects the estimates of the FUG method (Wankat, 2017). Furthermore, accurate estimates from FUG require the input of accurate relative volatility (Wankat, 2017).

Despite the limitations of the estimation, a shortcut column was simulated in DWSIM. The shortcut column provides a range of values that can be more or less expected and is used in order to reduce the amount of time spent trying to find the optimum column operation (Narváez-García *et al*, 2017; Ramapriya *et al*, 2018). The column was simulated to provide the desired product flow rate and composition for the bottoms and distillate, given the feed specifications. Table 7 provides the initial estimates that were taken from the shortcut column simulation.

Table 7: Initial estimates for the column optimisation

N_{min}	8
Feed stage	4
R_{min}	1.14

The initial estimates were then used as indication as to, more or less, where the column would operate. This allowed for a range of realisable values to be used in the sensitivity analysis. The sensitivity analysis was performed through the application of a ChemSep column in DWSIM. The reflux ratio and number of stages are of major consideration in

the design optimisation due to the fact that capital cost is highly dependent on these two variables (Gaurav, Ng & Rempel, 2016). It was therefore, selected that the first sensitivity analysis would be carried out in order to optimise the number of stages and reflux ratio. A higher reflux ratio and greater number of stages implies increased capital cost. The sensitivity analysis was based of the fact that complete separation of C_3's from C_4's was desired. Additionally, along with this desired separation was the desired flow rate of isobutene in the bottoms product (De Sousa Melim *et al*, 2020). The desired flow rate of the isobutene was $25\,878\,\mathrm{kg\,hr^{-1}}$. Figure 3 and Figure 4 illustrates a sensitivity analysis to obtain the desired flow rate while looping through different values for the reflux ratio and number of plates. The reflux ratio runs are shown as detailed in the given legend. The number of plates was selected as an independent variable (input) and the isobutene flow rate as a dependent variable (ouput). Figure 3 is used to show how the reflux ratio of 1 does not provide satifactory flow rate of product, while higher reflux ratios reach much closer to the desired flow rate. Figure 4 is then used to detail the most effective reflux ratio and number of stages for the desired flow rate.

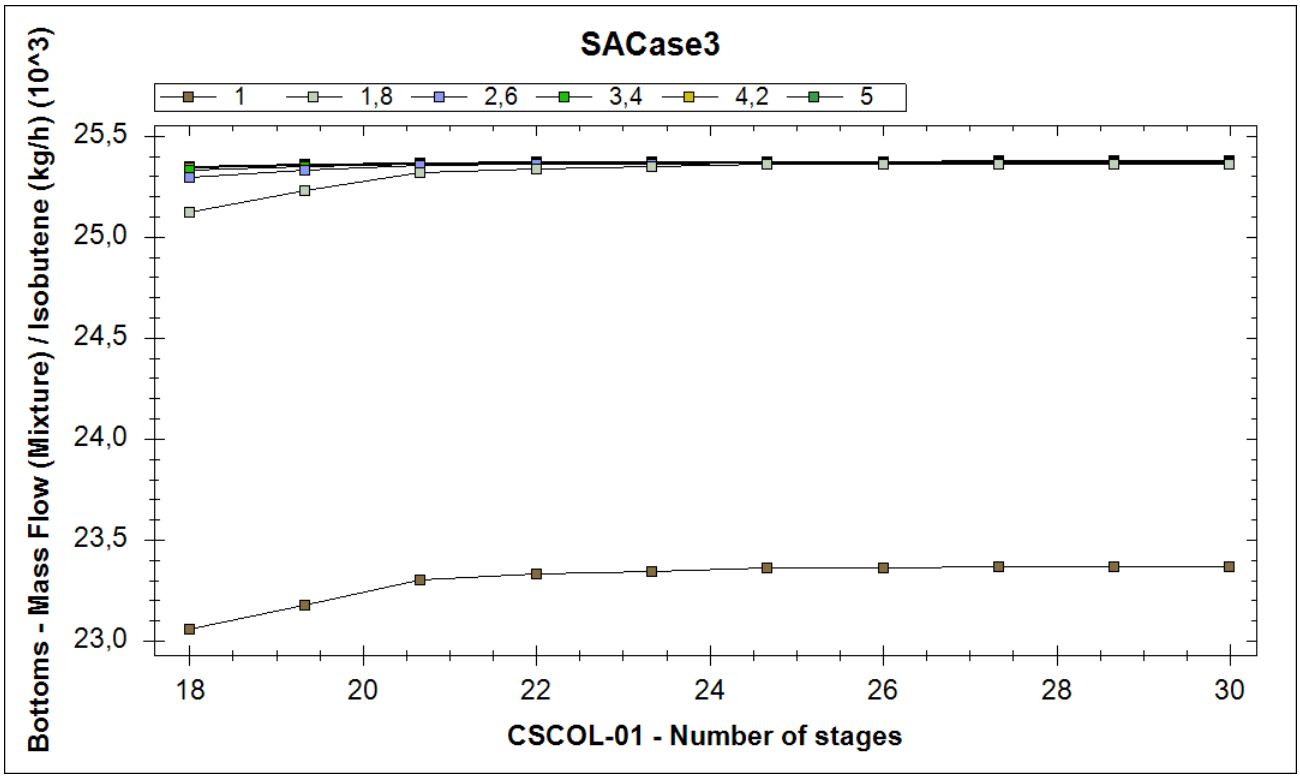

Figure 3: Sensitivity analysis for the isobutene flow rate

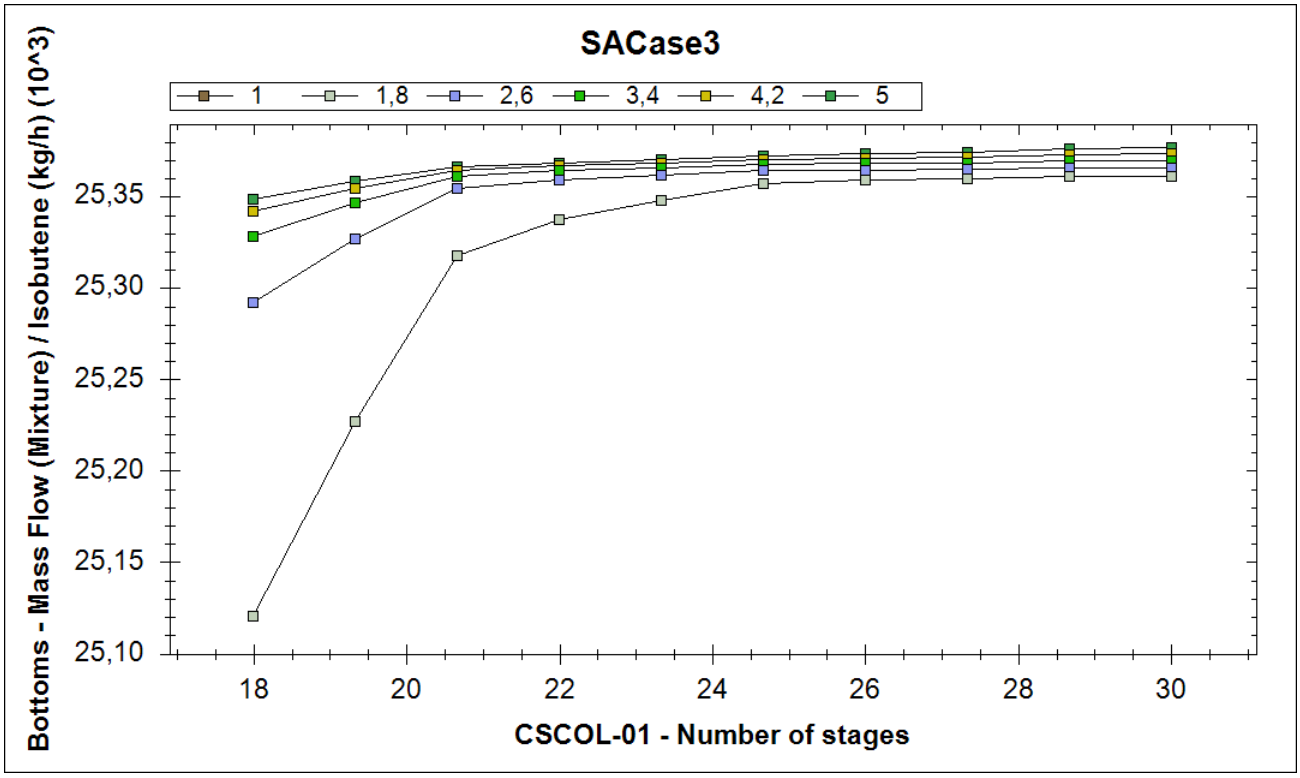

Figure 4: Detailed sensitivity analysis for the isobutene flow rate

The figures above provide good insight into being able to optimise the column. However, this flow rate sensitivity analysis needed support. Therefore, Figure 5, Figure 6, Figure 7 and Figure 8 provide detailed sensitivity analysis data. The figures allow for selection of the optimum number of stages and reflux ratio based on the best desired separation. The figures show the fraction of propane and propylene in the bottoms, the fraction of propane in the distillate and then the fraction of isobutene in the distillate, respectively. Figure 8 is used to ensure that minimal isobutene (desired reactant) is lost to the distillate. The desired amount of propane and propylene in the bottoms is 0. The number of stages was varied between 18 and 30 while the reflux ratio varied between 1 and 6.

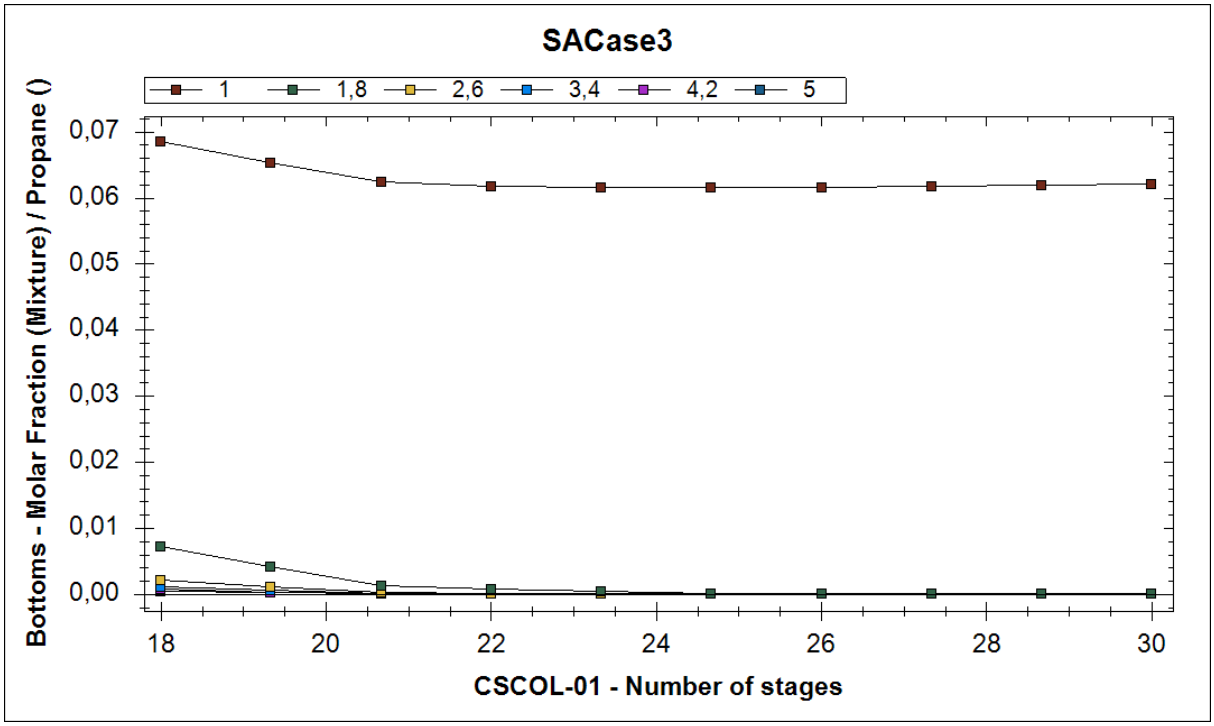

Figure 5: Sensitivity analysis for the fraction of propane in the bottoms product

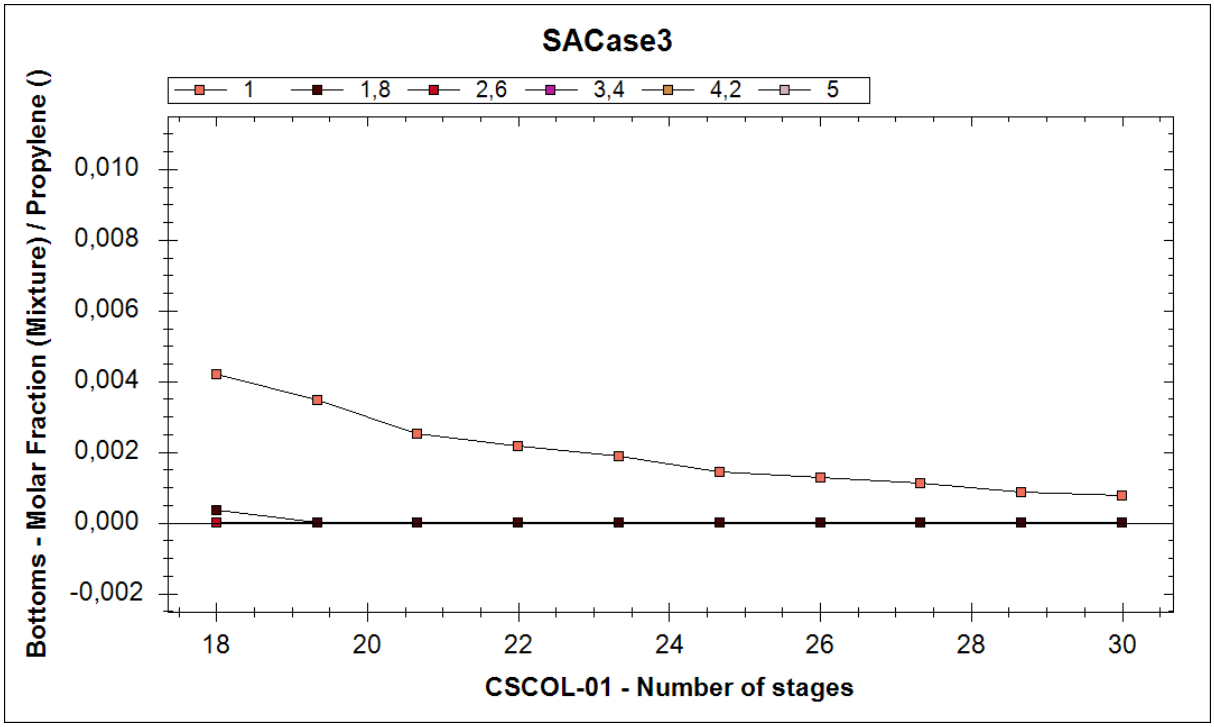

Figure 6: Sensitivity analysis for the fraction of propylene in the bottoms product

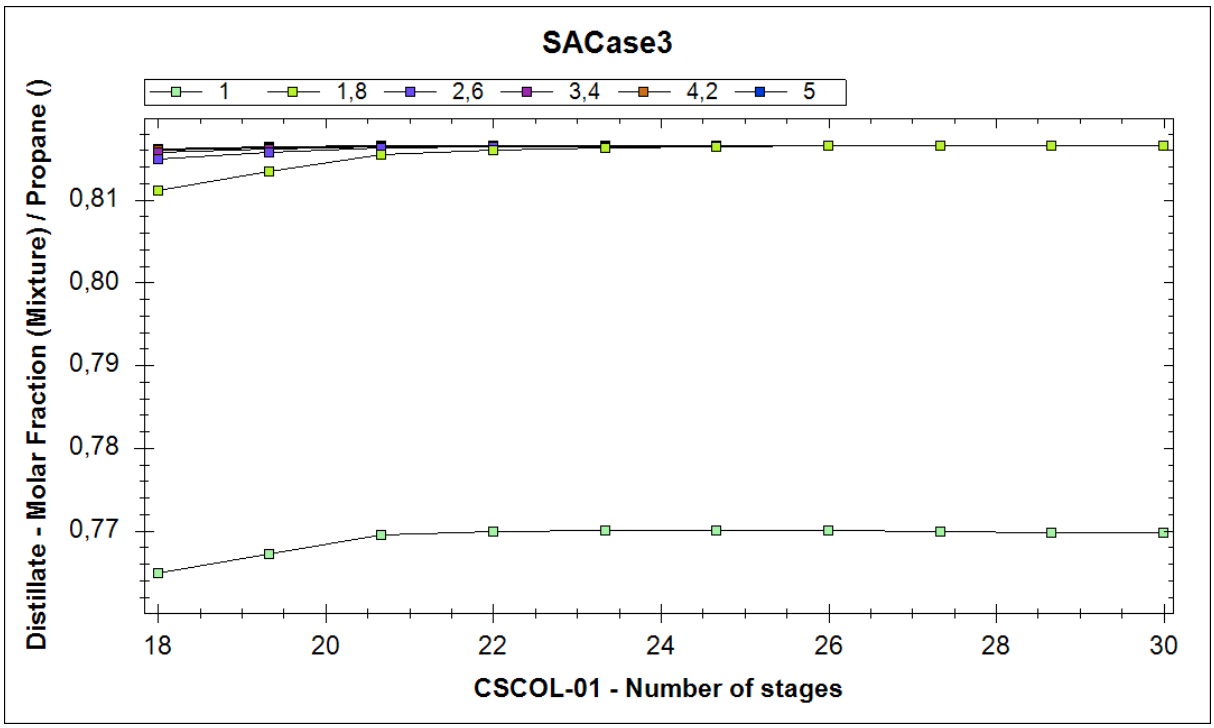

Figure 7: Sensitivity analysis for the fraction of propane in the distillate

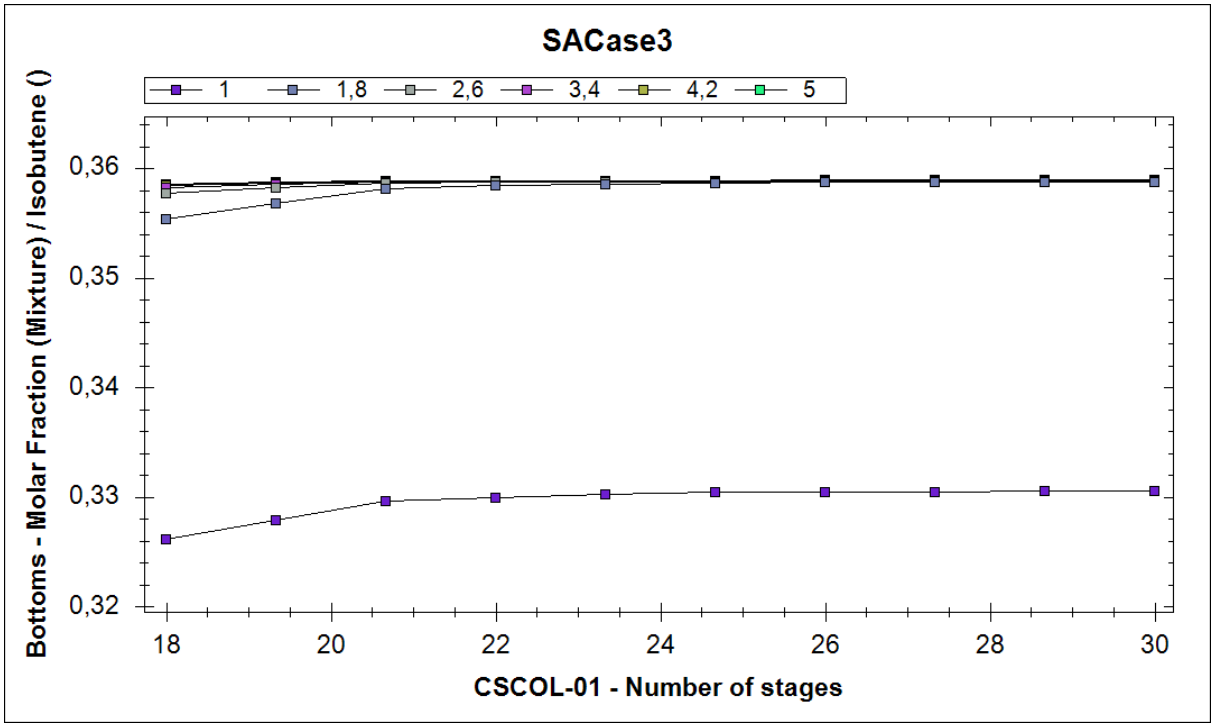

Figure 8: Sensitivity analysis for the fraction of isobutene in the distillate

The decision of optimum reflux ratio and number of stages was made with the desired flow and concentration parameters kept in mind. The desired separation is to have as little as possible (ideally, zero) C_3 compound in the bottoms while still maintaining a

flow rate of isobutene in the bottoms that was as near to 25 878 kg hr^{-1} as possible (De Sousa Melim *et al*, 2020). The number of stages and reflux ratio was optimised at 18 stages with a reflux at 1.8. These values were then used to simulate a rigorous column in DWSIM. The rigorous column was used to perform a manual sensitivity analysis to determine the optimum feed stage. Table 8 illustrates the sensitivity analysis conducted using the rigorous distillation column.

Table 8: Feed stage sensitivity analysis

N_{stages}	Feed stage	Reflux ratio	Isobutene mass flow (kg hr^{-1})	Propane bottoms mole fraction
18	10	1.8	25493	0.007
18	12	1.8	25423	0.011
18	11	1.8	25383	0.0176
18	9	1.8	24217	0.02
18	8	1.8	25703	0.0279
18	4	1.8	24720	0.05
18	14	1.8	24526	0.0674

The sensitivity analysis and design optimisation therefore, concluded in the column design as specified in Table 9. This table provides detail on the optimised column, simulated as a rigorous distillation column in DWSIM.

Table 9: Optimised column design simulated as a rigorous distillation column in DWSIM

Property	value
N_{stages}	18
Feed stage	10
Reflux ratio	1.8
Isobutene flow rate (bottoms)	25 493 kg hr^{-1}
Condenser duty	17 279 kW
Reboiler duty	−14 091 kW

The design optimisation for the desired high flow rate (De Sousa Melim *et al*, 2020) produced a trade off between reflux ratio and heat exchange duty. To reduce the heat exchange duty, the reflux ratio would have to increase dramatically, this would imply a larger column and increased capital cost. To keep the reflux ratio as close to the

minimum as possible the heat exchange duties become extremely large and the capital cost for the heat exchangers increases. However, the trade off is chosen such that, rather to design for larger heat exchangers than larger columns. This extremely high flow rate and large heat exchange duty and area is indicative of an error in judgement made during the group design (De Sousa Melim *et al*, 2020). The reason for choosing to design for a larger heat exchanger is that, perhaps the energy for heat exchange can be sourced from excess energy that is wasted else where on the plant. Since the production flow rate is so extremely high, it is inevitable to have high energy waste streams. Therefore, large heat exchange areas instead of large columns allows for the opportunity to use "second-hand" energy as this will reduce the operating cost of the heat exchangers. Furthermore, it is assumed that due to spatial arrangement, assuming the plant is in the open, the column height is not an issue. Therefore, the reflux ratio should not be made extremely high.

4 Column design and calculations

4.1 Efficiency

The mechanical design was done based off the optimised column design. The overall efficiency of the column is calculated using Equation 2 as described by Wankat (2017), with $\mu_{mixture}$ reported in cP.

$$E_o = 0.52782 - 0.27511log(\alpha_{\frac{LK}{HK}} \times \mu_{mixture}) + 0.044923[log(\alpha_{\frac{LK}{HK}} \times \mu_{mixture})]^2 \qquad (2)$$

The efficiency was calculated as 80.5 % and Table 10 provides adjusted design parameters for the column efficiency calculated. The high efficiency is attributed to the high relative volatility value for the light and heavy key distillation.

Table 10: Efficiency adjusted column design parameters

Property	value
N_{stages}	23
Feed stage	12
Reflux ratio	1.3
Boil-up ratio	2.3
Isobutene flow rate (bottoms)	$24\,917\,kg\,hr^{-1}$
Condenser duty	14 231 kW
Reboiler duty	−11 098 kW

4.2 Column considerations and constraints

The efficiency parameters allow for the design of an optimised, realistic multi-component distillation column. The type of distillation column selected for design is a plate distillation column. This is due to the relatively low complexity involved in the light and heavy key separation. Additionally, platted columns tend to be lighter in weight when compared to packed columns, this is effective with higher distillation columns (Wankat, 2017). The plate column decision was supported by the need for sufficient liquid distribution as packed columns tend to support maldistribution of the liquid in the column (Sinnott & Towler, 2019). The plated columns provide for simple design and ensure ease of maintenance, as well that packed columns are used for low capacities (ChemicalEngineeringWorld, 2019). The constraints to the column design is that the feed to the column is a two-phase mixture that is non-ideal. The column operates at a high pressure and relatively low temperatures. The column needs to be well insulated as operation is adiabatic. The column needs to be constructed from an inexpensive material, corrosion of the material of construction is not a major consideration as the hydrocarbon mixture is not considered highly corrosive (Santos, King, *et al*, 2008). This is true since there is a lack of water present, therefore, no corrosive acids can form (Esposito *et al*, 2017). The choice of a plated column implies that there are different types of tray designs available for selection. A sieve tray was selected for the tray design. The sieve tray is cost effective and allow for high capacities with constant flow rates (Sinnott & Towler, 2019). The material of construction for the column can either be carbon steel, stainless steel or titanium (Perry & Green, 2008). Since internal corrosion is not an issue, carbon steel is selected as material of construction. This material is inexpensive and will support adiabatic operation of the column. However, the trays should be constructed from type 304 stainless steel to support the weight of the column (Bander, 2012). Additionally, tray spacing decision

made was to select a tray spacing of 1.64 m (Wankat, 2017). This allows for crawl space in the event of tray and column maintenance. For columns of diameter greater than 3 m a tray spacing greater than 60 cm is recommended, since, heavy support beams restrict crawl space (Wankat, 2017). The material of construction for the condenser and reboiler was chosen as type 304 stainless steel as water is used as the cold and hot utility which makes the condenser and reboiler vulnerable to oxidation and corrosion.

4.3 Column dimensions

The column diameter for the plated distillation column is designed by choosing the bigger diameter for the column based of rectifying and stripping section diameters calculated. The diameter calculation procedure is adapted from (Sinnott & Towler, 2019). Calculation for the diameter of both the stripping and rectifying sections of the column are detailed below. The calculation begins with the liquid-vapour flow factor as shown in Equation 3.

$$F_{LV} = \frac{L}{V} \times \sqrt{\frac{\rho_V}{\rho_L}} \tag{3}$$

The above equation is used for the calculation of both bottoms and distillate liquid-vapour fraction, with densities and flows respective to the specific calculation. The calculation is complimented with simple distillation mass balances. The distillate reports $F_{LV} = 0.13$, while the bottoms has $F_{LV} = 0.34$. The flooding velocities for the distillate and bottoms are calculated, respectively, using Equation 4.

$$u_f = K_1 \times (\frac{\sigma}{0.02})^{0.2} \times \sqrt{\frac{\rho_L - \rho_V}{\rho_V}} \tag{4}$$

With a plate spacing chosen as 1.64 m in Section 4.2 a value for the constant (K_1) was read off the graph provided in Sinnott & Towler (2019: 568). The flooding velocities for the distillate and bottoms were calculated as $0.29\,\mathrm{m\,s^{-1}}$ and $0.22\,\mathrm{m\,s^{-1}}$, respectively.

According to Sinnott & Towler (2019), a good heuristic is to design for 85 % flooding at maximum velocity. Therefore, distillate and bottoms design velocity is reported as $0.25\,\mathrm{m\,s^{-1}}$ and $0.18\,\mathrm{m\,s^{-1}}$, respectively. The maximum flow velocities are used to calculate the net area required, knowing the maximum vapour mass flow rate and density for distillate and bottoms. Equation 5 details the total area required for separation.

$$A = \frac{\dot{m}}{\rho \times u_V} \tag{5}$$

The area for the rectifying section was calculated as $7.5\,\mathrm{m}^2$ and the stripping section area as $8.9\,\mathrm{m}^2$. Sinnott & Towler (2019), suggest that initial trial be done using the downcomer area as 12 % of the net area. Therefore, new required area from rectifying and stripping section is $8.5\,\mathrm{m}^2$ and $10.1\,\mathrm{m}^2$, respectively. This implies that, using standard column geometry, the diameter of the rectifying and stripping section is 3.3 m and 3.6 m, respectively. Thus, the column diameter is chosen:

$$D_c = 3.6\,\mathrm{m}$$

This, relatively, large column diameter is owed to the high flow rate designed for in the group report ($47\,\mathrm{kg\,s^{-1}}$ of vapour in the rectifying section and $45\,\mathrm{kg\,s^{-1}}$ vapour flow in the stripping section) (De Sousa Melim *et al*, 2020).

The maximum volumetric liquid flow rate was calculated as $0.13\,\mathrm{m^3\,s^{-1}}$. The high liquid volumetric flow rate suggests the use of a single pass plate as described in Sinnott & Towler (2019: 581). Table 11 shows detail of the design up to this point. According to Sinnott & Towler (2019), for a preliminary downcomer correlation of 12 %, a good estimate for the weir length is 77 % of the column diameter. Sinnott & Towler (2019), further elaborates on preliminary selection of weir sizing, recommending, weir height, hole diameter and thickness. It is to be noted, the plate material of construction is stainless steel as mentioned in Section 4.2. The values presented in Table 11 are aligned with recommendations provided by Sinnott & Towler (2019). Specifically, careful attention was given to the suggested values for the plate dimensions and ensured that the selected values aligned with design recommendations made by Sinnott & Towler (2019).

Table 11: Column dimensions

Property	unit	value
Column diameter (D_c)	m	3.6
Column area (A_c)	m^2	10
Downcomer area (A_d)	m^2	1.2
Net area (A_n)	m^2	8.8
Active area (A_a)	m^2	7.6
Hole area (A_h)	m^2	0.38
Weir length (L_w)	m	2.8
Weir height	mm	40
Hole diameter (d_h)	mm	3
Plate thickness	mm	3

To validate the diameter design, a weeping test was conducted, detailed in Sinnott (2014) which is symmetric to the weeping test followed by Wankat (2017). The minimum weeping liquid rate is used as 70 % of the maximum liquid flow rate. Therefore, the minimum height of the liquid crest is calculated using Equation 6, the minimum liquid flow rate is used (L_{min}):

$$h_{ow} = 750 \times [\frac{L_{min}}{\rho_L \times L_w}]^{0.67} \tag{6}$$

Equation 7 shown below, is used to determine the minimum vapour velocity at the weep point (Sinnott & Towler, 2019). However, before this equation can be used, a value for the constant needs to be determined. This value is determined from a graph provided in Sinnott & Towler (2019: 571) where the weir height and crest height are summed to a value 118 mm. This value determines the independent variable and thus, a K_2 value can be read off the graph. The K_2 value is estimated as: $K_2 = 31.1$ (Sinnott & Towler, 2019).

$$\breve{u}_h = \frac{K_2 - 0.9(25.4 - d_h)}{\rho_v^{0.5}} \tag{7}$$

The minimum vapour velocity at the weep point was calculated to be $\breve{u}_h = 2.1\,\mathrm{m\,s^{-1}}$. Equation 8 shown, calculates the actual minimum vapour velocity. Here, V_{max} refers to the volumetric maximum vapour flow rate:

$$\check{u}_{min} = \frac{0.7 \times V_{max}}{A_h} \tag{8}$$

Equation 8 results in $\check{u}_h = 3.4\,\mathrm{m\,s^{-1}}$. Therefore, it can be concluded that since the actual minimum vapour velocity is well above the weep point minimum vapour velocity, weeping will not be an issue.

The hole pitch ($\mathrm{L_p}$) is suggested by Sinnott & Towler (2019) to be a minimum of 2 hole diameters. Equilateral trianglar patterns are selected for the hole layout. This layout is chosen at it is the most common layout used in industry as well as it provides the highest and most constant efficiency (Wankat, 2017). A hole pitch is selected as c.a 3.8 diameters (Wankat, 2017) ($L_p = 12\ mm$). The number of holes is calculated with knowledge of the net hole area and the diameter of a single hole. The number of holes in the triangular layout is estimated at 54 000 holes.

Additional testing was done through, plate pressure drop, downcomer liquid back-up, entrainment and flooding, investigation. The total plate pressure drop is calculated using Equation 9 (Sinnott & Towler, 2019).

$$h_t = h_d + h_w + h_{ow_{max}} + h_r \tag{9}$$

Table 12 details the values used in the calculation of the total plate pressure drop as well as the final plate total pressure drop calculated for the design.

Table 12: Pressure drop calculation variable values

Property	unit	value
$\mathrm{\check{u}_h}$	$\mathrm{m\,s^{-1}}$	4.9
$\mathrm{h_d}$	mm	103
$\mathrm{h_r}$	mm	25.6
$\mathrm{h_{ow_{max}}}$	mm	98.4
$\mathrm{h_t}$	mm	266.6
ΔP_{plate}	kPa	1.3

The plate pressure drop calculation led to the downcomer liwuid back-up calculation which incorporates flooding consideration (Sinnott & Towler, 2019). Table 13 details the design parameters used to determine the downcomer liquid back up and pressure drop.

These calculations were based off the procedure provided by Sinnott & Towler (2019: 583).

Table 13: Downcomer liquid back-up and residence time calculation variable values

Property	unit	value
h_{ap}	mm	30
A_{ap}	m^2	0.084
h_{dc}	mm	416
h_b	mm	821
h_{check}	mm	840
t_r	s	7.4

To avoid flooding, h_b must be less than h_{check}, $h_{check} = 0.5(\text{tray spacing} + h_w)$. This holds true when the minimum area between A_{ap} and A_d is chosen. Therefore, flooding is avoided. Furthermore, the residence time is greater than 3 s, as suggested by Sinnott & Towler (2019). The final mechanical design is to evaluate entrainment. Table 14 details the calculated variables for the entrainment test. The table was generated using graphical correlations found in Sinnott & Towler (2019: 570).

Table 14: Entrainment calculation variable values

Property	unit	value
u_v	$m\,s^{-1}$	0.21
Percent flooding	%	72.5
F_{LV}		0.34
ψ		0.004

The value of $\psi = 0.004$ as calculated in Table 14 is well below $\psi = 0.1$ (Sinnott & Towler, 2019).

Once all the tests have been satisfied and mechanical design complete, the simple calculation to determine the column height (H_{column}) can be performed. Equation 10 (Wankat, 2017) was used for the calculation of the column height, where t_{tray} is the specified tray thickness, S is the tray spacing and N is the actual number of stages.

$$H_{column} = (N - 2)(t_{tray} + S) \tag{10}$$

The column height was calculated to be 35 m. The high column is a result of a large tray spacing correlation to the number of stages chosen for optimum design. This height, however, is not unrealistic. Since the column is to be built out in the open, the height of the column is not a major concern. The height of the column is strongly influenced by the high feed flow rate to the column designed by De Sousa Melim *et al* (2020).

It is to be mentioned that preliminary design parameters suggested by Sinnott & Towler (2019) resulted in weeping. Therefore, the weir height, hole area, hole diameter and thickness for the plate were adjusted. Sinnott & Towler (2019) suggests a hole diameter of 3 mm for stainless steel plates. Additionally, Sinnott & Towler (2019) suggest the weir height have a lower bound of 40 mm while the whole area has an initial trial value taken as 10 % of the active area. However, engineering judgement and design decision led to the selection of the hole area as 5 % of the active area.

4.4 Insulation

The column insulation ensures adiabatic operation of the column and functions as a corrosion protection layer for the carbon steel column since the column external is built outdoors and will be exposed to the atmosphere. Therefore, Fibreglass is selected as the insulation material. Fibreglass has an estimated thermal conductivity of $0.04\,\mathrm{W\,m^{-1}\,K^{-1}}$ and density in the region of $41\,\mathrm{kg\,m^{-3}}$ (Nave, 2020). Fibreglass application is quick and easy, with the fibreglass applicable to the external surface of the distillation column. This also allows for ease of maintenance of the insulation. Fibreglass is a non-combustible material that is readily available and inexpensive compared to other insulators. The wall thickness of the distillation column adds some support to the insulation while strengthening the structure. Therefore, standard sizing for carbon steel was selected which implied decision of a wall thickness of 6 mm. Furthermore, the insulation thickness was selected to be 60 mm (U.S Department of Energy, 2020), further adding to the rigidity of the structure.

5 Heat exchangers

5.1 Condenser

The condenser is design to be a single shell pass and four tube pass, shell and tube heat exchanger. Using water as the cooling utility implies that water enters at 303.15 K and

leaves the heat exchanger at 313.15 K, this (due to the large duty of the condenser) results in a relatively "unrealistic" heat exchange area as determined by engineering judgement. The distillate is cooled from 335 K to 316 K as stipulated by DWSIM (De Sousa Melim *et al*, 2020). Sinnott & Towler (2019), provide approximation for the overall heat transfer coefficient for a hydrocarbon mixture. Sinnott & Towler (2019) suggest a range from 350 to 900 $\mathrm{W\,m^{-2}\,K}-1$ for a hydrocarbon hot fluid with cooling water used as the cold fluid. Conservative design would be to design for the minimum heat exchange area necessary and this would, therefore, imply selection of the maximum value for the overall heat transfer coefficient.

$$U = 900\,\mathrm{W\,m^{-2}\,K^{-1}}$$

Equation 11 is applied to the calculation of the heat exchange area.

$$\dot{Q}_{cond} = U \times A_s \times \Delta T_{lm} \tag{11}$$

with

$$\Delta T_{lm} = \frac{(T_{h,in} - T_{c,out}) - (T_{h,out} - T_{c,in})}{ln(\frac{T_{h,in} - T_{c,out}}{T_{h,out} - T_{c,in}})}$$

obtained from Yunus (2019) for a counter flow heat exchanger. General circle geometry is assumed for the area of heat exchange.

The standard piping length was used as suggested by Greef I.L (2000). A inner tube diameter was chosen at 25 mm with a tube thickness of 5 mm. The normal stock length of piping was chosen as 6 m (Greef I.L, 2000). This design choice was based on standard piping sizes available, according to Greef I.L (2000). The thinner the tube implies a better assumed heat transfer. The choice of piping size enable volume and number of tube estimation. Table 15 details the mechanical design for the condenser.

Table 15: Condenser mechanical design parameters using cooling water as cold utility

Property	unit	value
Q_{cond}	kW	17 279
$\dot{m}_{\text{cooling water}}$	kg s^{-1}	413
$T_{h,in}$	K	335
$T_{h,out}$	K	316
$T_{c,in}$	K	303.15
$T_{c,out}$	K	313.15
ΔT_{lm}	K	17
U	$\text{W m}^{-2}\,\text{K}^{-1}$	900
As	m^2	1057
$d_{t_{inner}}$	mm	25
$d_{t_{outer}}$	mm	30
t_{wall}	mm	5
L_{tube}	m	6
N_{tubes}		2244

The number of tubes needed for the heat exchanger is significantly large, as is for the area of heat exchange, when cooling water is used as the cold utility. This is due to the trade-off discussed in Section 3. A better and more expensive alternative would be to use a refrigerant for the cold utility of the condenser. A common refrigerant used in condensers is R134a (freezing point – 164 K). If it is assumed that R134a is available at 173.15 K as a subcooled liquid, with a boiling point of around 246 K, the heat exchange area drastically improves. However, the area is still large. Table 16 details the heat exchange parameters using R134a that leaves the heat exchanger at 313 K.

Table 16: Condenser mechanical design parameters using R134a as cold utility

Property	unit	value
Q_{cond}	kW	17 279
$T_{h,in}$	K	335
$T_{h,out}$	K	316
$T_{c,in}$	K	173.15
$T_{c,out}$	K	313.15
ΔT_{lm}	K	65
U	$W\,m^{-2}\,K^{-1}$	900
As	m^2	291
$d_{t_{inner}}$	mm	25
$d_{t_{outer}}$	mm	30
t_{wall}	mm	5
L_{tube}	m	6
N_{tubes}		618

5.2 Reboiler

The most cost effective reboiler is a thermosyphon reboiler (Sinnott & Towler, 2019). This type of reboiler has a relatively high thermal conductivty. It is for these two reasons why a horizontal thermosyphon reboiler is chosen as the type of reboiler, since the reboiler duty is extremely high at c.a -11000 kW (owing to the high flow rate designed for in the group design (De Sousa Melim *et al*, 2020)). The hot utility is steam available at 2200 kPa while the properties for the cold utility is taken as similar to the properties for isobutene (main component in bottoms). Sinnott & Towler (2019: 745) provides an algorithm for the solution of the mechanical design of a thermosyphon reboiler. This algorithm was followed and the results from the calculation are provided in Table 17.

Table 17: Horizontal thermosyphon reboiler mechanical design parameters

Property	unit	value
Q_{reboil}	kW	-11 098
Mean overall ΔT	kW	157
T_r	K	1.45
Design heat flux	$W\,m^{-2}$	47 300
As	m^2	235
$d_{t_{inner}}$	mm	25
$d_{t_{outer}}$	mm	30
t_{wall}	mm	5
L_{tube}	m	2.44
N_{tubes}		1037

The reboiler, similar to the condenser, has a high duty as mentioned in Section 3. This implies that the large heat exchange area and volume boils down to the fact that the high flow rate fed to the column requires high heat exchange duty in order for the column to be design as realisable as possible. Section 3 mentions the design decision as to why larger heat exchange area was chosen over increased column size.

6 Design Detail

This section of the report details drawings and dimensions to visually aid the mechanical design. The column support is chosen to be a standard straight skirt constructed from stainless steel to protect the skirt from corrosion. The material of the skirt and column are easily weld together. Figure 9 shows the chosen design for the skirt support with manhole access structure. Additionally, internal support is required for the sieve trays. The stainless steel sieve trays are supported as shown in Figure 10. The sieve trays spacing is designed in order to support the weight of the sieve trays with the large column diameter that is designed.

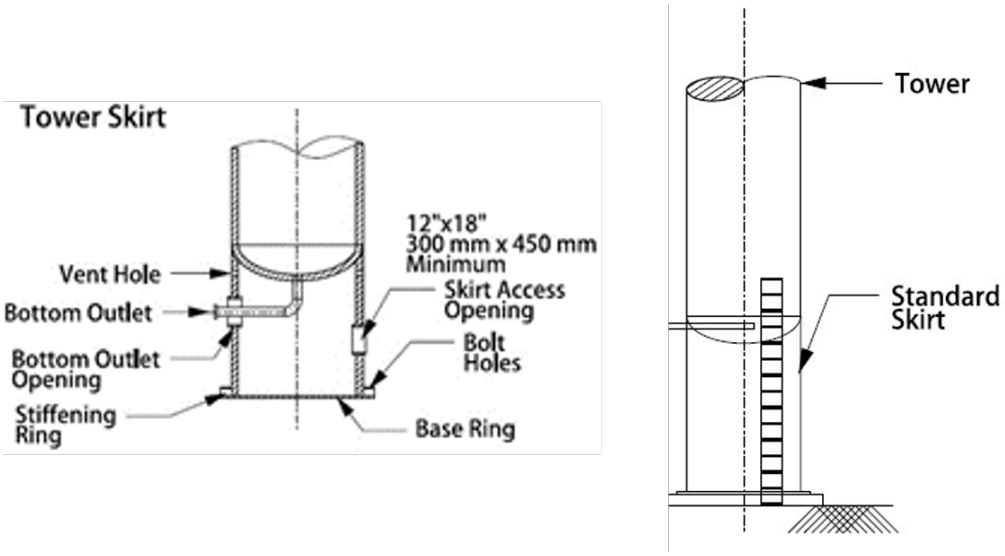

Figure 9: Stainless steel standard straight skirt for distillation column support (PipingEngineer, 2015)

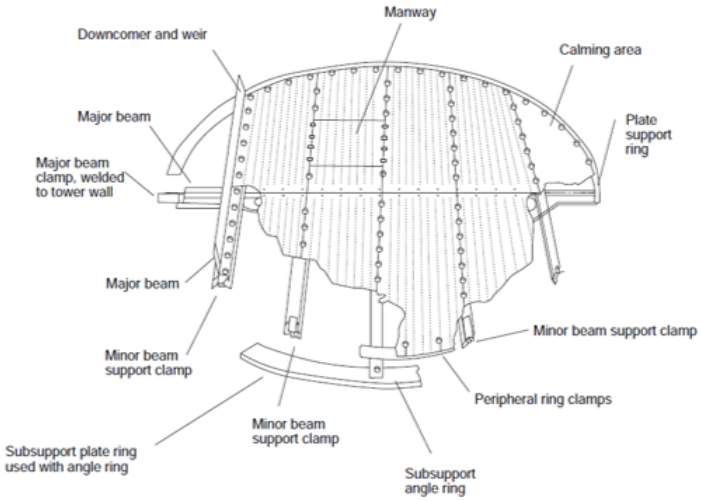

Figure 10: Stainless steel sieve tray internal support (Sinnott & Towler, 2019)

Internal column dimensions and plate hydraulics are detailed in Figure 11 and Figure 12. Figure 11 shows the equilateral triangular hole pitch selected as well as the pitch length. Figure 11 also demonstrates the hydraulics and phenomena possible on the plate and in the downcomer (Sinnott & Towler, 2019). The figure includes dimensions for the active area and tray spacing.

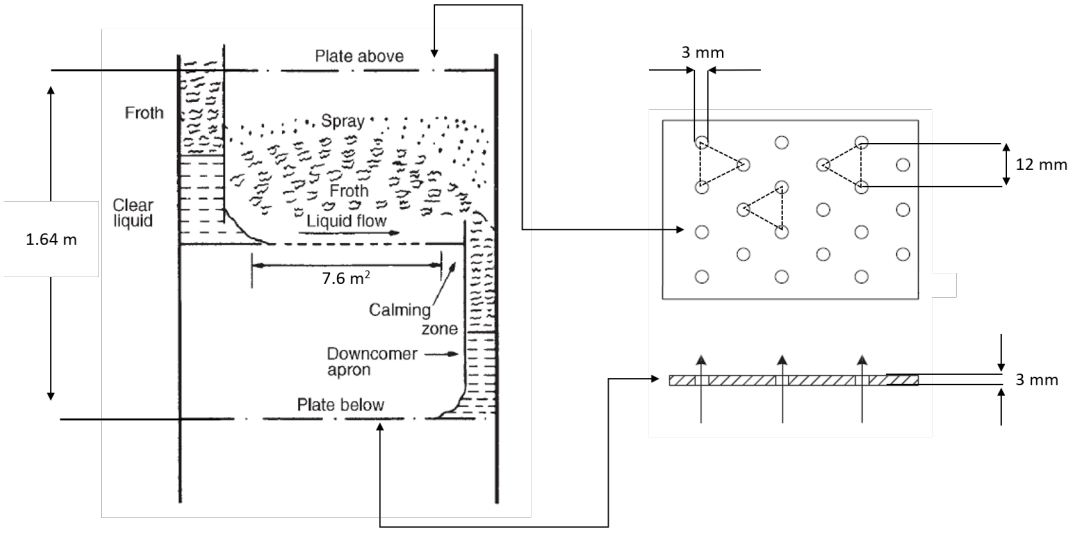

Figure 11: Plate hydraulic illustration and dimensions, adapted from Sinnott & Towler (2019)

Figure 12 provides a detailed mechanical design visual for the weir and downcomer. Dimensions of the weir, such as height, length and plate thickness, are shown in the figure. Additionally, the downcomer area is detailed in a *top view* representation of the weir and downcomer.

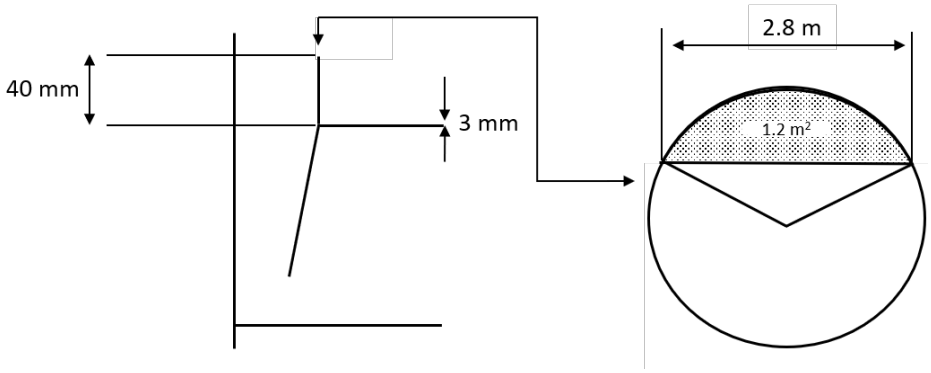

Figure 12: Weir and downcomer dimensions, adapted from Wankat (2017)

7 References

Bander, F (2012) *Separation technologies* URL: `http://seperationtechnology.com` (visited on 10/08/2020).

ChemicalEngineeringWorld (2019) *Packed column versus tray column* URL: `https://chemicalengineeringworld.com/packed-column-versus-tray-column` (visited on 10/08/2020).

De Sousa Melim, G, Lazenby, M, Pouroullis, E, Scheepers, J and Steenekamp, G (2020) *A design for producing ethyl tert-butyl ether (ETBE) from petroleum sourced LPG and renewably sourced ethanol* tech. rep. Department of Chemical Engineering, University of Pretoria, South Africa.

Esposito, RO, Alijó, PHR, Scilipoti, JA and Tavares, FW (2017) *Compositional grading in oil and gas reservoirs*, Gulf Professional Publishing.

Gaurav, A, Ng, F and Rempel, G (June 2016) "A New Green Process for Biodiesel Production from Waste Oils via Catalytic Distillation using a Solid Acid Catalyst - Modelling, Economic and Environmental Analysis" *Green Energy Environment*, *1*, DOI: 10.1016/j.gee.2016.05.003.

Greef I.L, SW (2000) *Piping System Design*, Department of Chemical Engineering University of Pretoria.

McKinsey (2020) *LPG* URL: https://www.mckinseyenergyinsights.com/resources/refinery-reference-desk/lpg (visited on 08/11/2020).

Narváez-García, A, Zavala-Loría, J, Ruiz Marin, A and Canedo, Y (June 2017) "Short-Cut Methods for Multicomponent Batch Distillation" in: ISBN: 978-953-51-3201-1 DOI: 10.5772/66830.

Nasri, Z and Housam, B (Mar. 2009) "Applications of the peng-robinson equation of state using MATLAB" *Chemical Engineering Education*, *43*, 115–124.

Nave, C (2020) *Thermal conductivity.*

Perry, RH and Green, DW (2008) *Perry's chemical engineers' handbook*, 8th ed. McGraw-Hill, New York ISBN: 9780071422949.

PipingEngineer (2015) *Distillation tower elevation and support* URL: https://www.pipingengineer.org/distillation-tower-elevation-and-support (visited on 10/09/2020).

Ramapriya, GM, Selvarajah, A, Jimenez Cucaita, LE, Huff, J, Tawarmalani, M and Agrawal, R (2018) "Short-Cut Methods versus Rigorous Methods for Performance-Evaluation of Distillation Configurations" *Industrial & Engineering Chemistry Research*,

57, (22): 7726–7731 DOI: 10.1021/acs.iecr.7b05214 URL: https://doi.org/10.1021/acs.iecr.7b05214.

Santos, B, King, F, *et al* (2008) "Corrosion Of Carbon Steel In Petrochemical Environments" in: *CORROSION 2008* NACE International.

Sinnott, R (2014) *Chemical engineering design*, vol. 6 Elsevier.

Sinnott, R and Towler, G (2019) *Chemical engineering design: SI Edition*, Butterworth-Heinemann.

U.S Department of Energy (2020) *Types of Insullation* URL: https://www.energy.gov/energysaver/weatherize/insulation/types-insulation (visited on 10/09/2020).

Wankat, PC (2017) *Separation process engineering*, Pearson Education.

Yunus, AC (2019) *Heat and mass transfer: fundamentals and applications*, McGraw-Hill Education.